COOLING EFFECT OF A MEMS BASED MICRO CAPILLARY PUMPED LOOP FOR CHIP-LEVEL TEMPERATURE CONTROL

Jeffrey Kirshberg
Berkeley Sensor and Actuator Center, University of California at Berkeley
497 Cory Hall
Berkeley, CA 94720
Phone: (510) 642-4876, Fax: (510) 643-6637, Email: jkirsh@newton.berkeley.edu

Kirk Yerkes
Air Force Research Laboratory AFRL/PRPG
Wright-Patterson AFB, OH
Phone: (937) 656-4428, Fax: (937) 656-4132, Email: yerkeskl@wpafb.af.mil

Dave Trebotich and Dorian Liepmann
Berkeley Sensor and Actuator Center, University of California at Berkeley
497 Cory Hall
Berkeley, CA 94720
Phone: (510) 642-9360, Fax: (510) 642-5835, Email: liepmann@me.berkeley.edu

ABSTRACT

Utilizing current Micro Electro Mechanical Systems (MEMS) technologies, a three-port micro-capillary pumped loop (micro-CPL) was designed, fabricated and tested to provide integral cooling to electronics or MEMS type devices. The two wafer design consists of one silicon and one borofloat glass wafer. An analytical study was used in determining the geometry of the device, including the evaporator dimensions (1000 μm x 2000 μm) and the length of the liquid and vapor lines (35 mm). Using laser spot heating, the finished device was run near steady-state. It was determined that the micro-CPL resulted in a backside cooling effect of at least 7 C when a laser delivering 7.5 W (+/- 0.2 W) with a spot-size diameter of 1.0 mm was focused on the front side of the evaporator region.

NOMENCLATURE

A_c	= condenser surface area
A_w	= cross-sectional area of wick
c_p	= specific heat
D	= diameter
f	= friction factor
h	= groove height
h_c	= condenser convection coef.
h_{fg}	= latent heat of vaporization
K	= wick permeability
L	= length
$\dot{m}$	= mass flow rate
N_g	= groove number
P	= pressure
ΔP_c	= capillary pressure
ΔP_l	= liquid pressure losses
ΔP_t	= pressure due to temp. difference
ΔP_v	= vapor pressure losses
ΔP_w	= pressure losses in wick
Q	= power
r_c	= capillary radius
r_h	= hydraulic radius
R	= gas constant
Re	= Reynolds number

T = temperature
v = velocity
w = groove width
w_t = total groove structure width
a = groove aspect ratio
e = wick porosity
m = viscosity
r = density
s = surface tension

Subscripts
c = condenser
e = evaporator
l = liquid
v = vapor

INTRODUCTION

In general there are many challenges in transitioning MEMS technologies to specific applications such as micro-coolers. Specific technical challenges to the development of a micro-cooler include; (a) identification of potential micro-cooler thermodynamic processes, components, and geometries, (b) addressing the physics of micro scale heat transfer in solids, vapor, and liquids specific to micro-cooler geometries, (c) addressing the physics of phase change phenomena in the micro scale regime, (d) the development of macro scale to micro scale scaling laws specific to micro-cooler fluid systems, (e) addressing system level benefits as well as interfacing between the micro- to the macro-world, (f) modification of current or the development of new fabrication processes to allow the micro-cooler to be charged with the appropriate working fluid during fabrication, and (g) the development of appropriate calibration and testing diagnostics to verify micro-cooler performance.

There are numerous potential configurations for consideration when developing a micro-cooler. A micro-cooler may make use of micro scale phase change or single phase heat transfer to reject heat from electronics packages such as miniature heat pipes (Peterson, et al. 1993) (Hoelke, et al. 1999). Regardless of configuration, an effective micro-cooler will have to be able to fully control the movement of fluids throughout the system. The combination of micro scale heat transfer and fluid dynamics along with high surface to volume ratios will make the development of an efficient micro-cooler a challenging endeavor.

The conceptual design and fabrication of a micro-CPL was first presented by Kirshberg, et al. (1999). It encompasses the initial design of a completely passive three-port micro-CPL, schematically shown in Figure 1. It is important to realize that micro-devices can support extremely high gradients because of their small size. The evaporator region will be placed in direct contact with the micro-processor, sensor, or other electronic chip for which cooling is required and used to maintain an optimal temperature. The advantages of this approach are three-fold, first, precise temperature control at the chip-level, second, the overall cooling is more efficient because specific heat sources within the electronics package may be targeted, third, the overall size of the electronic system can be kept small.

Not only do CPLs offer greater geometric freedom over traditional heat pipes, but they can carry much greater heat loads due to the co-current nature of the vapor and liquid flows, as opposed to the counter-current flows in conventional heat pipes (Faghri, 1995). Another distinct advantage of the CPL is the potential to further enhance the device's performance. Major components of the system may consist of a new family of pumps and valves to control liquid or vapor transport within the micro-CPL as well as innovative micro scale heat acquisition and heat rejection regions. These regions may incorporate micro-mixers potentially using enhanced surfaces to promote heat transfer, condensation, and boiling.

This paper is a continuation of Kirshberg, et al. demonstrating the first operational micro-CPL of which the authors are aware. Initial analyses are supported by experimental and numerical results.

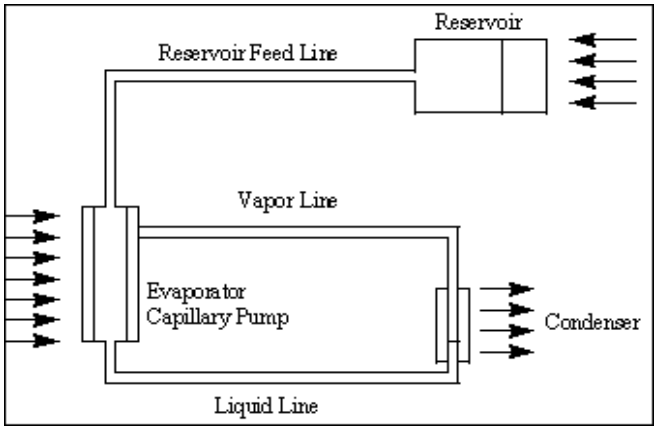

Figure 1. *Schematic of a micro-CPL.*

ANALYSIS

Table 1 provides specifications for a micro-CPL with rectangular liquid/vapor line cross-sectional geometries, in addition to a planar evaporator and condenser with a grooved capillary wicking structure. An analysis of the micro-CPL Capillary Pumping Limit was conducted following the rationale of Dickey and Peterson (1994) but including the pressure drop of the vapor line.

Evaporator Length	2000 μm
Evaporator Width	1000 μm
Condenser Area	2.0e+06 sq. μm
Groove Height	50 μm
Groove Width/ Number	50 μm / 8
Vapor Line Width	150 x 450 μm
Liquid Line Width	150 x 150 μm
Vapor/Liquid Line Length	35 mm
Liquid Line Re Number	42
Vapor Line Re Number	488
Projected Heat Removal	4 Watts

Table 1. Micro-CPL specifications.

This relationship was iteratively solved for the micro-CPL mass flow

$$\dot{m}^2\left(\frac{c_p h_{fg}}{A_t h_t}\right)+\dot{m}\left[h_{fg}+c_p T_s-\left(\frac{c_p Q_t}{A_t h_t}\right)-c_p T_{w,c}\right]-Q_t=0 \qquad (1)$$

$$\bar{v}=\frac{\dot{m}}{rA} \qquad (2)$$

while maintaining the following pressure relationship.

$$\Delta P_c + \Delta P_t \geq \Delta P_w + \Delta P_l + \Delta P_v \qquad (3)$$

Each pressure term in the above relationship represents a particular geometric portion of the micro-CPL for which the pressure balance must be maintained for proper CPL operation. The liquid and vapor lines were treated as rectangular ducts. The remainder of the pressure terms are assumed to have the following macro-scale relationships:

Capillary pressure drop,

$$\Delta P_c = \frac{2s}{r_c} = \frac{2s}{w} \qquad (4)$$

Pressure drop due to the temperature gradient across the wick using the Clausius-Clapeyron equation,

$$\Delta P_t = \frac{h_{fg} P_v \Delta T}{R T_v^2} \qquad (5)$$

Liquid line pressure drop (rectangular duct) (Blevins, 1984),

$$\Delta P_l = r\left(\frac{64}{\mathrm{Re}_l\left(\frac{2}{3}+\frac{11}{24}\left(\frac{h_l}{w_l}\right)\left(2-\frac{h_l}{w_l}\right)\right)}\right)\left(\frac{L_l}{D_l}\right)\left(\frac{\bar{v}_l^2}{2}\right) \qquad (6)$$

Vapor line pressure drop (rectangular duct),

$$\Delta P_v = r\left(\frac{64}{\mathrm{Re}_v\left(\frac{2}{3}+\frac{11}{24}\left(\frac{h_v}{w_v}\right)\left(2-\frac{h_v}{w_v}\right)\right)}\right)\left(\frac{L_v}{D_v}\right)\left(\frac{\bar{v}_v^2}{2}\right) \qquad (7)$$

Pressure drop across the wick structure,

$$\Delta P_w = \int_0^{L_e}\frac{m_l \dot{m}_l}{r_l A_w K}dx = \int_0^{L_e}\frac{m_l Q}{r_l h_{fg} A_w K}dx = \frac{m_l Q L_e}{r_l h_{fg} A_w K} = \frac{m_l Q L_e \left(f_l \mathrm{Re}_l\right)(2h+w)^2}{8 r_l h_{fg} N_g (hw)^3} \qquad (8)$$

The macro-scale auxiliary relationships of wick permeability,

$$K = \frac{2e r_{h,l}^2}{f_l \mathrm{Re}_l} = \frac{8w(hw)^2 N_g}{f_l \mathrm{Re}_l w_t (2h+w)^2} \qquad (9)$$

hydraulic radius,

$$r_{h,l} = \frac{2hw}{2h+w} \qquad (10)$$

wick porosity,

$$e = \frac{hwN_g L_e}{A_w L_e} = \frac{wN_g}{w_t} \qquad (11)$$

and the friction relationship,

$$f_l \mathrm{Re}_l = 24\left(1-1.3553a+1.9467a^2-1.7012a^3+0.9564a^4-0.2537a^5\right) \qquad (12)$$

were also used in this analytical approach.

RESULTS

Using water as a working fluid, assuming an operating temperature of 100 C and 3 degrees of sub-cooling with a condenser heat transfer coefficient of 10 W/m^2-C, the maximum transport length is shown in Figure 2. The results shown in Fig. 2 predict heat transport potential of 1.4e-01 W-m for the 35mm vapor/liquid lines.

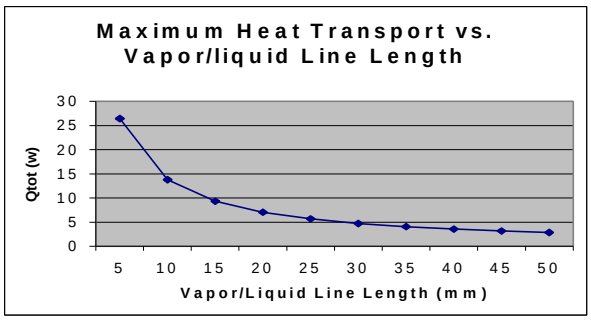

Figure 2. *Maximum transport distance for 150x150 micron liquid and 450 x 150 micron vapor lines.*

FABRICATION

Figure 3 illustrates the design of the micro-CPL. The evaporator, condenser and liquid/vapor lines are fabricated from a single crystal silicon wafer. The wicking structure consists of axial grooves wet etched into a standard borofloat glass wafer, which serves as a cover plate. Glass was chosen because of its transparent nature, however this wicking structure will eventually be etched directly into the backside of whatever electronic package requires cooling. A tube is connected to the backside of the silicon wafer via a through hole in order to function as the reservoir feed line. The reservoir is off-chip and pressurized, therefore controlling the operating temperature of the device.

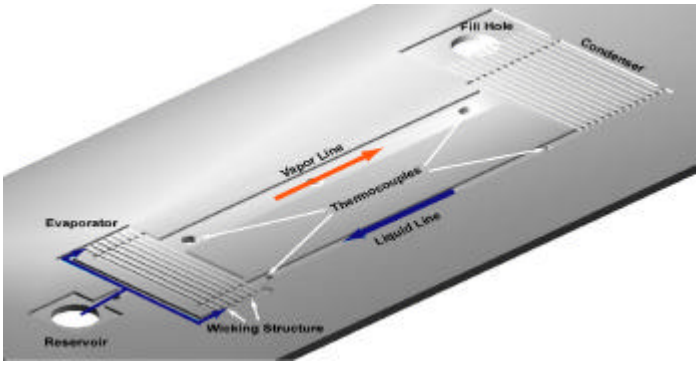

Figure 3. *A sketch of the micro-CPL. The fluidic channels (gray) are fabricated from silicon, while the wicking structure (white) is etched into a borofloat glass cover plate.*

The fabrication of the fluidic channels in the silicon wafer requires two separate deep reactive ion etches. Initially, 3µm of oxide were thermally deposited onto the wafer. A photoresist mask was then created on top of the oxide. The oxide was plasma etched in a Lam etcher in order to create an oxide mask for the wafer. 10µm of thick photoresist were then spun on top of the oxide mask, which once exposed, developed and baked, served as a mask for the through holes. A Surface Technology Systems deep reactive ion etcher was used to create the through holes. Once completed, the remaining photoresist was stripped thus revealing the oxide mask beneath it. The wafer was then deep trench etched 150µm, thus creating the fluidic channels. This process is outlined in Figure 4.

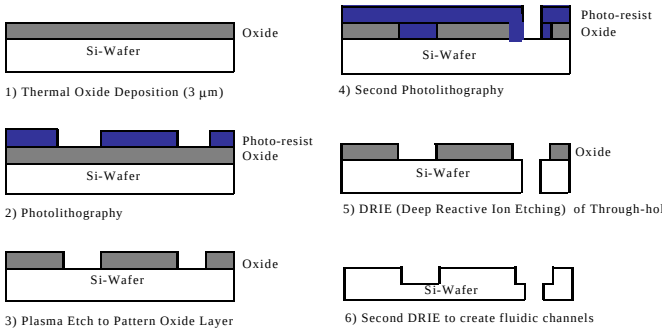

Figure 4. *Fabrication process for the silicon wafer*

The wicking structure is fabricated in the borofloat glass cover plate. 1 µm of undoped polysilicon was deposited on the glass wafer. A photoresist mask was then used when placing the wafer in CF_4 plasma. Once the silicon mask was complete, and the photoresist stripped, the wafer was placed in concentrated HF for 6 minutes. This isotropic etch created the parabolic channels, with radius of 50 µm, which function as the wicking structure in the micro-CPL. This process is outlined in Figure 5.

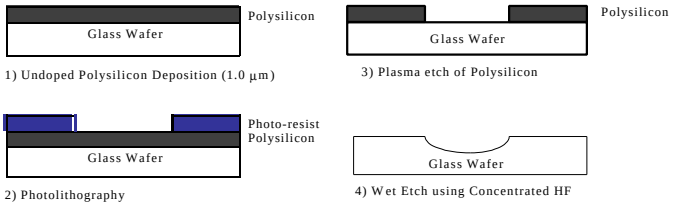

Figure 5. *Fabrication process for the glass wafer*

The two wafers are then cleaned, aligned and anodically bonded. The reservoir feed line is then attached to the through hole, which connects the micro-CPL to a pressurized reservoir. Figure 6 above shows SEMs of the now completed micro-CPL.

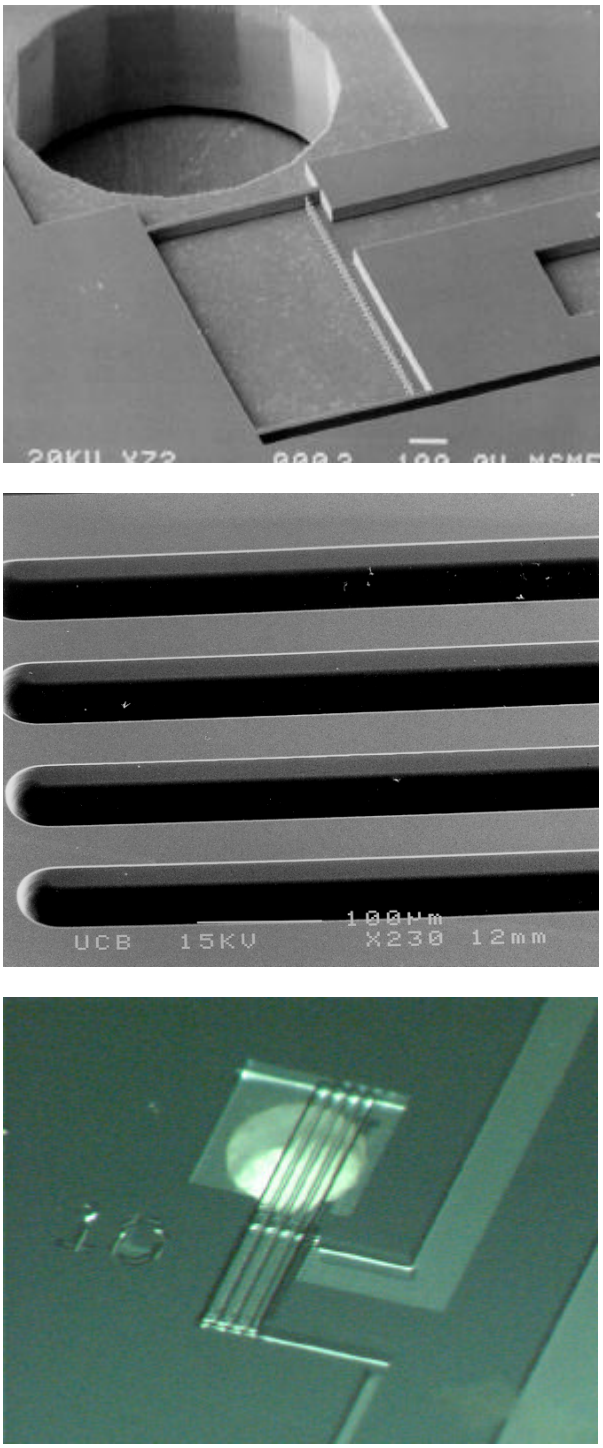

Figure 6. *(a) Top view of the condenser, plenum and fill-hole regions. (b) Axial grooves wet etched into glass cover plate. (c) Condenser region after anodic bonding to glass cover plate.*

EXPERIMENT

Initial preparation of the micro-CPL is quite similar to that of traditional CPLs. It must be pumped-down prior to filling in order to remove any air that might cause vapor-lock during operation. A turbo-pump was used in conjunction with

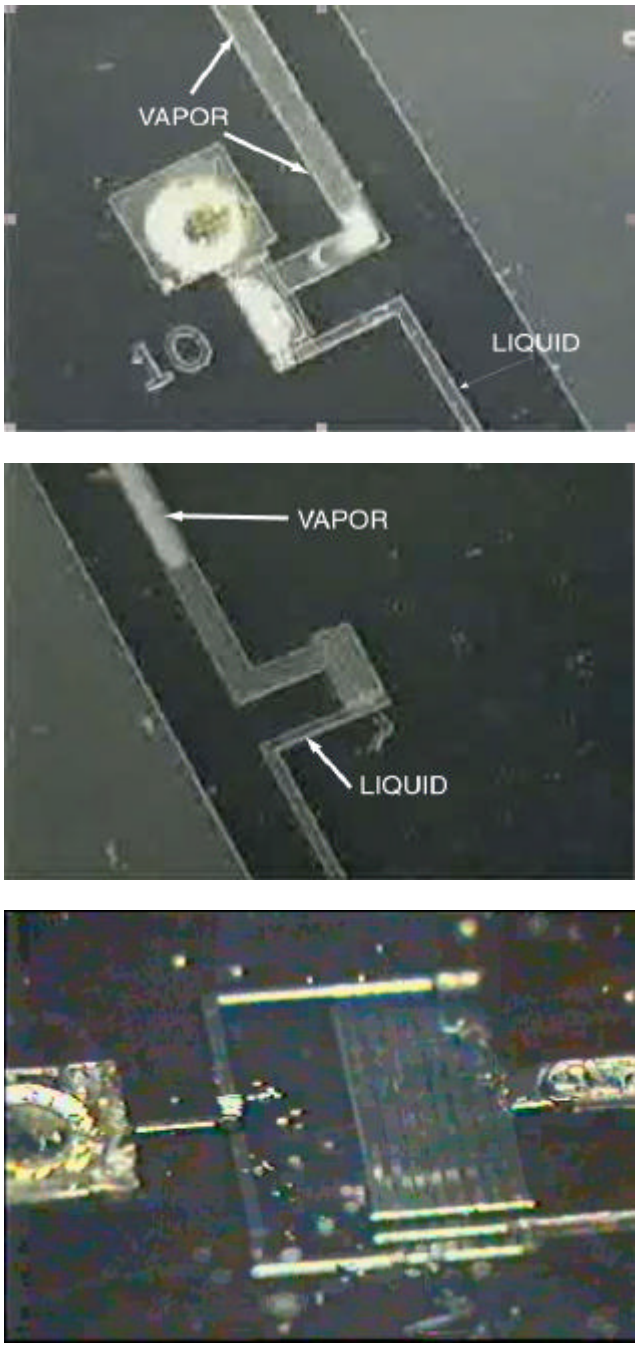

Figure 7*. (a) Evaporator region and (b) Condenser region of a previously reported (Kirshberg, et al. 1999) micro-CPL while operating at steady state. (c) Evaporator of Micro-CPL reported in this paper.*

the extra through-hole in the condenser region towards this end. The device was then flooded, and the reservoir pressurized to 15 psi above ambient. After filling the device successfully, the vapor line was cleared with a hand-held micro-torch. Heat is then applied to the evaporator region. Pictures of micro-CPLs operating continuously are shown in Figure 7.

In order to gain quantitative insight into the operation of the micro-CPL, the following experiment was set-up and performed. A CO_2 laser with a spot size diameter of 1.0mm was used to heat three different wafer configurations. First, a standard 100 mm diameter borofloat glass wafer with 500 μm thickness was anodically bonded to a double-polished p-type silicon wafer with similar dimensions. The laser spot was focused on the glass wafer at a point 20 mm away from the edge of the wafer, and 30mm away from the center of the wafer. Three thermocouples were then placed on the backside of the silicon wafer. The first thermocouple, referred to as "Center" was placed directly underneath the laser spot (30 mm away from the center of the wafer). The remaining thermocouples were placed at distances of 19 mm and 45 mm away from the center of the wafers along the same line as the first thermocouple, and are referred to as "Inboard" and "Outboard" respectively. It was determined that a laser power of 7.5 W (+/- 0.2 W) resulted in a "Center" temperature of just above 100C.

Two similar tests were then performed on an identical set of anodically bonded glass and silicon wafers, with the noted exception that a micro-CPL was now fabricated between the wafers. The micro-CPL was not insulated and the condenser exposed to quiescent room air. The evaporator region of the micro-CPL lies 30 mm from the center of the wafer, at the "Center" point. When the micro-cooler was filled with air (no working fluid), a laser power of 7.5 W (+/- 0.2 W) resulted in a "Center" temperature of 78 C (+/- 1.0 C). Finally, the micro-CPL was filled with water and pressurized. Due to the latent heat of vaporization and sensible heating occurring within the filled micro-CPL, an identical laser power resulted in a lower "Center" temperature of 71 C (+/- 1.0 C). Figure 8 illustrates these experiments, while Figure 9 shows the resulting temperature profiles.

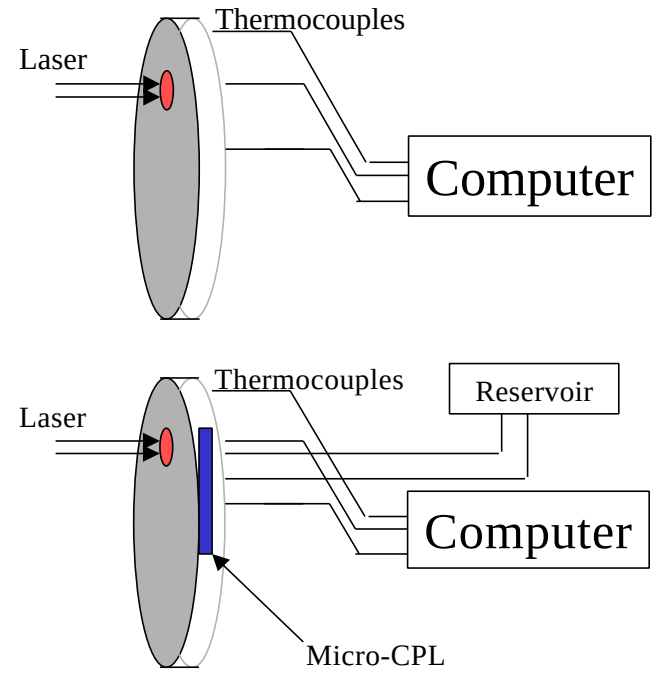

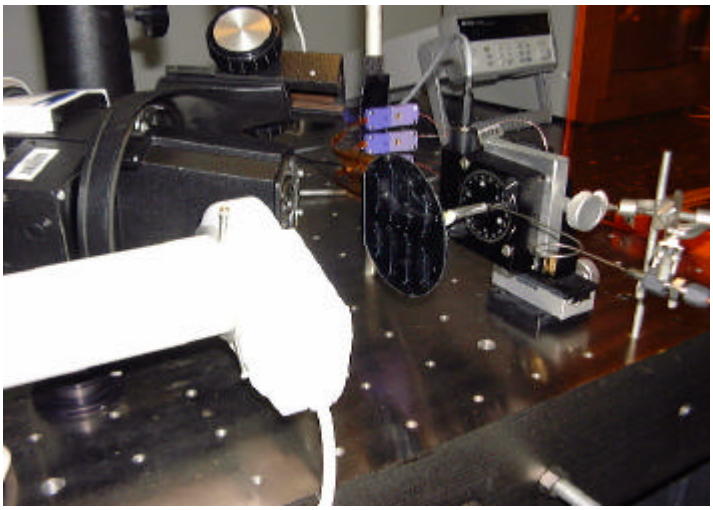

Figure 8. *(a) A schematic of the blank wafer (b) and the micro-CPL experiment, as well as (c) a picture of the experiments utilizing laser spot heating and thermocouples.*

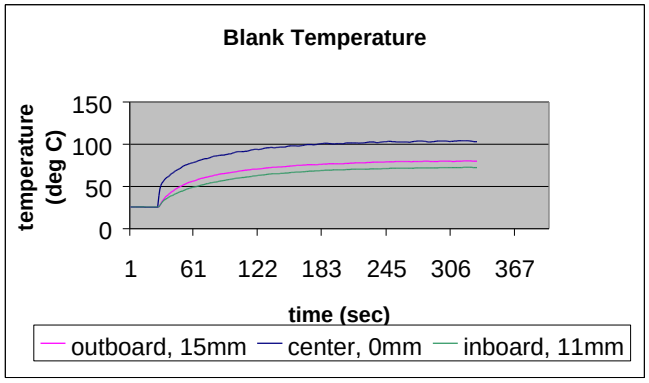

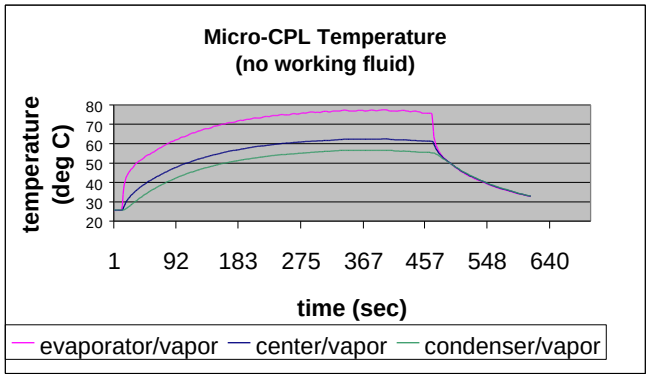

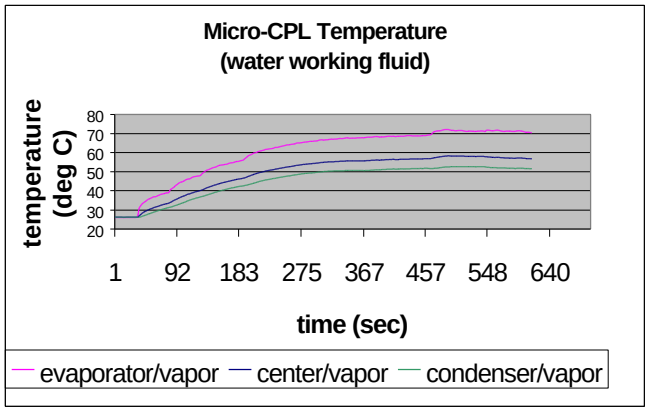

***Figure 9**. Temperature profiles for the (a) blank wafers (b) micro-CPL filled with air (no working fluid) and (c) micro-CPL filled with water.*

NUMERICAL ANALYSIS

Utilizing CFDRC's code, a two-dimensional axi-symmetric finite difference model, similar to that of the blank wafer experiment, was constructed. The model differed from the experiment in two ways. First, in the numerical model, the laser spot was simulated as being placed in the center of the wafers (rather than 30mm from the center). Secondly, the heat flux delivered by the laser spot was significantly less in the numerical model, with a total laser power of only 4.2 W, and a spot size diameter of 3.5 mm. Imposing natural convection boundary conditions, the simulation was run until steady-state was reached. The results for the temperature profile of the center of the wafers are shown below in figure 10.

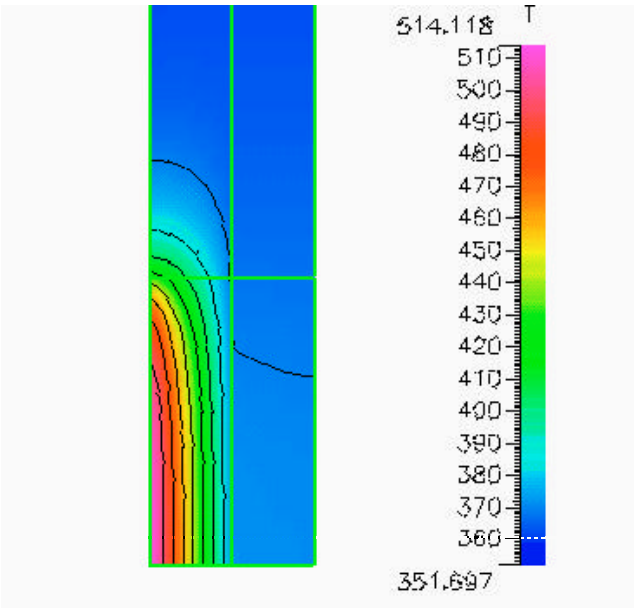

***Figure 10.** Temperature profile of a cross-section of the blank glass (left) and silicon (right) wafers. The bottom is the center of the wafer (where the heat source is placed on the glass side). Due to scaling, the outer sections of the wafers are not shown.*

This simulation solution showed a greater than 150 degree temperature differential along both axis when a 3.5 mm diameter laser spot of 4.2 W was applied at the glass surface. This resulted in a large temperature gradient in the glass due to the poor thermal conductivity of the glass. Heat spreading increased in a radial direction with an increase in incident laser power.

CONCLUSION

The micro-CPL provides at least 7 degrees of cooling to the backside of the device when a 7.5 W (+/- 0.2 W) laser spot with 1.0 mm diameter is placed on the front side of the evaporator region. This cooling effect is attributed to the micro-CPL's making use of the latent heat of vaporization and sensible heat of the fluid in the device. Due to the nature of electronic packages in general, this cooling effect might very well be used to optimize a device by allowing it to operate at lower temperatures.

With these preliminary numbers in hand, it is the author's task to optimize the micro-CPL and refine the experiments. In these experiments the condenser was allowed to run passively, yet it will enhance the micro-CPL's performance to spot cool the condenser (thus forcing condensation at an exact location while allowing for further sub-cooling of the liquid upon its return to the evaporator.) A vacuum chamber is being constructed so that the micro-CPL might be tested without convective heat losses to the ambient, in order accurately determine the maximum heat flux capacity of the device. Finally, due to the large temperature gradients that the micro-CPL can support, it is necessary to take temperature measurements inside the device rather than simply measure the backside. To this end, a thermal imaging system will also be employed.

ACKNOWLEDGMENTS

This research was begun under a grant from the Scientific and Technology Research Program for BMDO, and is now supported by DARPA under its HERETIC program. The fabrication was done at the Berkeley Sensor and Actuator Center, and would not have been possible except for the constant advice and support of its members. With the recent addition of Berkeley professors Ralph Greif and Costas Grigoropoulos, the project has already begun to move in exciting new directions. The finite difference code was supplied by CFDRC. The assistance and expertise of Don Reinmeuller in setting up the experiment at AFRL is thoroughly appreciated by the authors. And a special thanks to Ron Wilson for all his help with the SEMs.

REFERENCES

Blevins, R.D., 1984, Applied Fluid Dynamics Handbook,Van Nostrand Reinhold Company, New York.

Dickey, J.T. , and Peterson G.P. , 1994,"Experimental and Analytical Investigation of a Capillary Pumped Loop," *Journal of Thermophysics and Heat Transfer*, Vol 8, No. 3, pp. 602-607.

Faghri, A., 1995, Heat Pipe Science and Technology, Taylor & Francis, Washinton D.C.

Hoelke, A., Henderson, H.T., Gerner F.M., Kazmierczak, M., 1999 "Analysis of the Heat Transfer Capacity of a Micromachined Loop Heat Pipe," *Proceedings of the ASME Heat Transfer Division,* HTD-Vol. 364-3 pp. 53-60.

Kirshberg, J., Yerkes, K., and Liepmann, D., 1999 "Micro-Cooler for Chip-Level Temperature Control," SAE *Aerospace Power Systems Conference*, P-341.

Peterson, G.P., Duncan, A.B., and Weichold, M.H., 1993, "Experimental Investigation of Micro Heat Pipes Fabricated in Silicon Wafers," *Journal of Heat Transfer*, Vol 115, pp. 751-756.